The Enduring Legacy of Saturn V Launch Vehicle Flight Dynamics and Control Design Principles and Practices

Jeb S. Orr
Space Launch System Flight Dynamics and Control Technical Specialist
Mclaurin Aerospace, Huntsville, AL, jeb.orr@nasa.gov

John H. Wall
Space Launch System Ascent Flight Control Lead
Dynamic Concepts, Inc., Huntsville, AL, john.w.wall@nasa.gov

Cornelius J. Dennehy
Guidance, Navigation, and Control Technical Fellow
NASA Engineering and Safety Center, Greenbelt, MD, cornelius.j.dennehy@nasa.gov

Abstract

It has been over 50 years since the first launch of the Saturn V launch vehicle, Apollo 4, on November 9th, 1967. Developed at NASA's Marshall Space Flight Center (MSFC) in Huntsville, Alabama, the Saturn V was a massive multistage liquid-fuel expendable rocket used by NASA's Apollo and Skylab programs. It safely flew 24 American astronauts to the Moon, blazing the trail for all American heavy-lift launch vehicles to follow. The Saturn V remains the only launch vehicle to carry humans beyond low Earth orbit.
Nearly fifty years after the final May 1973 flight of the Saturn V, an enduring technical legacy of launch vehicle technologies still supports the United States's space launch capabilities, particularly with respect to flight dynamics and control. The structured refinment of GN&C technologies during the Saturn program, leveraging the incremental advancements of the Jupiter, Redstone, and Saturn I/IB, systematically reduced risk and resulted in the most advanced and reliable launch vehicle flight control systems to have been developed before the advent of the Space Shuttle.
Keywords: Saturn V, launch vehicles, flight control, flight dynamics, TVC, simulation

1. Introduction

The first uncrewed test flight of the Saturn V launch vehicle on November 9, 1967, AS-501, was the spectacular culmination of an immense program, begun in July 1960, that dedicated a majority of United States national aerospace resources to the development of a heavy-lift launch vehicle capable of bringing humans to the moon and back. Doing so required major advances in the technology of guidance, navigation, and control (GN&C), extending the fledgling state of early cold war ballistic missile GN&C technology that had theretofore been developed in response to a perceived Soviet strategic missile threat. NASA Marshall Space Flight Center (MSFC) managed and provided the technical leadership for the entire Saturn program, evolving it from earlier Army and NASA rocket programs conducted at MSFC and its predecessor, the Army Ballistic Missile Agency (ABMA).

A substantial portion the ABMA was transferred to the newly-formed National Aeronautics and Space Administration in November of 1959, which then assumed control of the Saturn vehicle development after it was begun by the Department of Defense's Advanced Research Projects Agency (ARPA) one year earlier.[1,2] An expert team of personnel recruited from the German rocket program under Operation Paperclip were placed under the leadership of Wernher von Braun at NASA Marshall. Other NASA centers, numerous universities, and the entirety of the national industrial aerospace infrastructure of the 1960's provided support to the Saturn program to create this soon-to-be iconic heavy lift launch vehicle.

The Saturn V launch vehicle (Figure 1.1) was a three-stage, liquid-propellant rocket vehicle consisting of the 5-engine LOX/RP-1 S-IC first stage produced by Boeing, the 5-engine LOX/LH2 S-II manufactured by North American-Rockwell, and the high-performance single-engine S-IVB third stage developed by McDonnell-Douglas. At liftoff, the Saturn V produced more than 7.6 million pounds (force) of thrust, with a fully loaded gross weight of 6.35 million pounds (mass).[3] At 363 feet in length, the Saturn V was a massive vehicle that shaped the development of NASA's ground handling facilities, and will remain unsurpassed in scale by any launch vehicle until the completion of the Space Launch System Block II cargo configuration by NASA in the coming decade.

The S-IC stage, with 345,000 gallons of liquid oxygen oxidizer and 216,000 gallons of RP-1 hydrocarbon fuel, comprised more than 5 million pounds of the total liftoff mass and 138 feet of the total vehicle length. The first stage burned for about two minutes and forty seconds, followed by an endoatmospheric staging and the ignition of the S-II stage, which continued the ascent for approximately six minutes, burning another 980,000 lbm of propellants. A final, two-and-a-half minute burn by the high-performance S-IVB placed the third stage and the Apollo spacecraft payload into an Earth parking orbit for systems checkout prior to a second translunar injection (TLI) burn performed by the S-IVB.[4]

Fig. 1.1: Saturn V Launch Vehicle (*Image: NASA*)

The Saturn program inspired a major advance, and more importantly, a standardization of the analytical methods and design practices for launch vehicle flight dynamics and control. Major contributions to the state of the art include now-common principles such as in-flight load relief, robust structural bending mode stabilization, and the use of linear and nonlinear mechanical analogs for sloshing propellant dynamics. The Saturn vehicles' analysis and certification process employed mathematically rigorous flight dynamics models for stability analysis, particularly with respect to structural bending, slosh coupling with the airframe, and statistical methods. Techniques such as Monte Carlo analysis, which are now considered fundamental to the design of all aerospace systems, were just coming of age as the aerospace industry witnessed the advent of hybrid analog-digital computation. A resourceful balance of intuition, first principles analysis, test validation, and engineering experience was applied to balance conservatism and meet the incredibly aggressive timeline of the Saturn vehicles' development.

GN&C and flight control hardware capability was likewise advanced. In the case of the Saturn launch vehicles, an approach derived from flight-proven hardware designs for then state-of-the-art ballistic missile guidance computers was employed for the launch vehicle digital computer (LVDC) and its associated adapter hardware. This was in contrast to the revolutionary integrated circuits applied in the development of the Apollo guidance computers (AGC) used on the Apollo spacecraft and lunar module (LM). However, there occurred the noteworthy development of the precision, high-power mechanical feedback hydraulic Thrust Vector Control (TVC) system, which laid the groundwork for the quad-redundant actuators used in the Space Transportation System (STS) Shuttle Orbiter vehicle and the Space Launch System (SLS) heavy lift launch vehicle.

Finally, GN&C autonomy played a unique, transitional role that permanently shaped the relationship of human crews to their space launch vehicles in the following decades. The Saturn vehicles were the first human-rated launch vehicles whose ascent guidance was executed on the vehicle itself, a marked departure from the Mercury-Redstone and Gemini (Titan II) Launch Vehicle (GLV) whose steering commands were computed on the ground and telemetered via radio uplink during the ascent phase.* The Saturn V included the first-ever automatic abort functionality, called the Emergency Detection System (EDS), which utilized high-reliability sensors to autonomously protect the crew in the event of an anomaly whose time-to-criticality exceeded the capabilities of human response. Finally, the Saturn V was interfaced cooperatively with its spacecraft payload, supporting human-

*The Titan II ICBM used an onboard inertial guidance system, but it was designed for ballistic trajectories and had a concerning reliability record at the time the Gemini program was instantiated.

in-the-loop navigation and ascent guidance redundancy through a limited manual steering interface.

This paper will provide an overview of the Saturn V GN&C technologies and highlight the multiple flight dynamics and control related technical innovations that emerged from the Saturn V launch vehicle project. The paper will also summarize and describe the particular launch vehicle design principles and practices that have endured since the 1960s, citing specific examples of their application in the GN&C design process for the ongoing SLS Program.

2. The Saturn V GN&C System

The Saturn V guidance, navigation, and control functionality was developed at Marshall Space Flight Center in the early 1960's under the supervision of the MSFC Astrionics Laboratory. Most of the technology was in its infancy as of the late 1950s, where it had been employed by the ABMA in the development of the Jupiter and later the Redstone ballistic missiles. The Redstone later evolved into the first American human-rated suborbital space vehicle, the Mercury-Redstone. These efforts were in parallel to, and quite separate from, the Apollo spacecraft GN&C hardware and software development being conducted at the Charles Stark Draper Laboratory, then called the MIT Instrumentation Laboratory, in Cambridge, Massachusetts.

The Saturn V GN&C hardware and software was essentially identical to, and had been extensively flight proven, on the earlier Saturn IB launch vehicle. The Saturn IB was a workhorse of the technology development and test program, facilitating incremental testing of subsystems prior to their first all-up demonstration on the Saturn V in 1967.

The Saturn V GN&C architecture consisted primarily of the ST-124M-3 inertial measurement unit, a separate flight control rate gyro assembly (RGA), the Launch Vehicle Data Adapter (LVDA), the Launch Vehicle Digital Computer (LVDC), and the Flight Control Computer (FCC) (Figure 2.1). Flight control feedback relied on digital attitude error commands resolved from the inertial platform and computed in the LVDC, along with analog rate feedback from the strapdown, triple-redundant rate gyro assembly whose reliability goals required the use of 9 independent gyroscopes. The Saturn IB also included accelerometer feedback for load relief, which was deleted from the Saturn V for reasons to be discussed in Section 4.1.

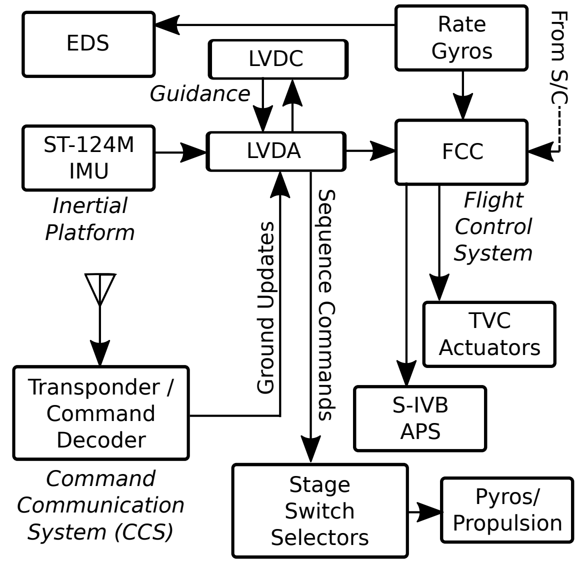

Fig. 2.1: Saturn IB/V Guidance, Navigation, and Control Architecture (*adapted from NASA MSFC IV-4-401-1*)

The entirety of the Saturn V avionics, telemetry, and vehicle management hardware was housed in a massive 21.7 foot diameter, 3 foot long structural ring known as the Instrument Unit (IU), manufactured by IBM in its Huntsville facility under contract to MSFC. The IU was located at the separation plane of the second and third stages. Since the IU not only contained the GN&C hardware but also supported the entire weight and bending loads of the third stage and payload, it was a significant structural member in its own right; it comprised about 4,300 lbm of the injected mass. The IU also contained a sophisticated thermal conditioning system using methanol-water coolant, a preflight inert gas purge system, hazardous gas detection equipment, and the supply system for the inertial platform gas bearings.[3] Its forward location allowed its use for the control of all three stages, including on-orbit operations.

2.1 *Inertial Platform and Rate Sensors*

The ST-124M-3 was a self-contained, 3-gimbal inertially stabilized platform developed during the Apollo program for the Saturn launch vehicles' boost guidance inertial reference functionality,[5] having evolved from a prior 4-gimbal design to minimize mass and maximize reliability. It employed three gas bearing gyroscopes and three pendulous integrating gyro accelerometers (PIGAs). The output of the gimbal resolvers and the integrated accelerations (inertial velocity) were supplied to the LVDA for signal conditioning and interfacing with the LVDC (for guidance) and FCC (for flight control). In addition, the platform angles were communicated to the Apollo spacecraft to drive the attitude director indicator (ADI) instrument and provide the spacecraft crew with abort cues and supplemental flight dynamics information. The total weight of the platform assembly, less its power supply, signal conditioning electronics, and gas bearing pressurization system, was about 112 lbm.

While "strapdown" inertial navigators had been developed and were in use at that time, including the Abort Guidance System (AGS) used on the Apollo Lunar Module, the state of the art for boost guidance applications was (and still is) a stable platform containing PIGAs. As the platform orientation was fixed in inertial space, the vehicle attitude was determined directly from the platform gimbal resolvers. In contrast, body attitude rates were not available directly from the stable platform; thus, the Saturn vehicles used a second, high-reliability strapdown rate gyro assembly colocated in the IU. This instrument package was also used as a primary indicator for the emergency detection system, discussed in the following section.

Initial alignment of two input axes of the ST-124M-3 was coplanar with the launch azimuth, so as to simplify, for example, the transformations required to measure crossrange path deviation during guidance computations. Initial azimuth alignment was performed with respect to the surveyed Earth reference azimuth using a theodolite located near the launch facility, and automatic platform leveling (to within 2.5 arcsec) was accomplished using two supplementary gas bearing pendulums to detect the local gravity vector. The gimbal resolvers provided an accuracy of about 20 arcsec at an angular rate of about 12 degrees per second, which was more than sufficient for accurate attitude control of the vehicle. PIGA accuracy was on the order of 5 cm/s per count. Post-calibration gyro bias (due primarily to temperature sensitivity) was limited by active thermal control of the IMU housing using the aforementioned IU liquid cooling system to not more than about 0.05 deg/hr.

2.2 *LVDC, LVDA, and EDS*

Navigation and guidance computations were performed digitally in the LVDC, and the LVDA served essentially as a high-reliability consolidated signal processing, data acquisition, and analog-to-digital conversion subsystem. The LVDA was a serial data processor having 512 kbit/s bandwidth with interfaces to the telemetry and ground control subsystems, stage switch selectors, and the LVDC using a 10-bit data bus. The LVDC contained a fixed-point processor with a 2 MHz clock, an effective instruction rate of about 12 kHz, and 114 kilobytes of random access, nonvolatile (core rope) memory. Compared with contemporary computers, the LVDC had less performance than most modern embedded microcontrollers.[†] The LVDC was engineered for exceptionally high reliability, avoiding the then-unproven integrated circuit approach in favor of triple-redundant, voted semiconductor modules called unit logic devices (ULDs). The LVDC weighed approximately 75 lbm and consumed 150W of power, while the LVDA, containing most of the signal processing equipment for the entire vehicle, weighed 214 lbm and consumed 320W of power.[5]

The principal function of the LVDC was execution of Iterative Guidance Mode (IGM), the first use of onboard closed-loop ascent guidance on a human-rated launch vehicle. IGM provided a near-optimal solution to the ascent vehicle two-point boundary value problem, recognizing that a considerable simplification could be obtained under the assumption that the tangent of the optimal thrust direction is a linear function of time.[6] This concept, known as a linear tangent guidance (LTG), became the basis of the subsequent development of Powered Explicit Guidance (PEG). PEG was used throughout the Space Shuttle program and is now implemented for use on Space Launch System.[7]

The Saturn V also implemented the first ever autonomous abort capability, known as the Emergency Detection System (EDS). The EDS included triple-redundant, majority-voted abort logic that was able to initiate engine shutdown and automatic crew escape under conditions whose time-to-criticality was generally assessed to be beyond the crew's reaction and decision time. The crew, however, retained the ability to inhibit automatic EDS operation at any time via switches in the spacecraft. These conditions included excessive angular rates (as measured by the IU-mounted rate gyros) and two-engine-out, both of which could indicate and/or lead to an immediate loss of control resulting in vehicle structural failure during atmospheric boost. The S-IVB stage used a triplex "hot wire" structural failure indicator for automatic initiation of the escape sequence if two out of three failures in any of three structural load paths were detected in flight (a total of 9 systems).

2.3 *Flight Control Computer*

The Flight Control Computer (FCC) was an entirely analog signal processing device, using relays controlled by the Saturn V Switch Selector Unit to

[†]As of this writing, a typical embedded processor, e.g., the PIC32MX12, provides 32-bit processing at 40 MHz and 256 KB of data storage at a unit cost of about USD $4.

manage internal redundancy and filter bank selection. The FCC contained multiple redundant signal processing paths in a triplex configuration that could switch to a standby channel in the event of a primary channel comparison failure. The flight control computer implemented basic proportional-derivative feedback for thrust vector control during powered flight, and also contained phase plane logic for control of the S-IVB auxiliary propulsion system (APS).

For powered flight, the FCC implemented the control law

$$\beta_c = a_0 H_0(s)\theta_e + a_1 H_1(s)\dot{\theta}$$

where a_0 and a_1 are the proportional and derivative gains, and $H_0(s)$ and $H_1(s)$ are the continuous-time transfer functions of the attitude and attitude rate channel structural bending filters, respectively. In the Saturn V configuration, the gains a_0 and a_1 were not scheduled; a discrete gain switch occurred. The Saturn V FCC also implemented an electronic thrust vector cant functionality using a ramp generator that vectored the S-IC engines outboard approximately 2 degrees beginning at 20 seconds following liftoff, in order to mitigate thrust vector misalignment sensitivity.[5]

2.4 Actuation Systems

The Saturn V used a robust set of thrust vector control effectors developed primarily at MSFC, using a mechanical feedback hydraulic actuator that implemented the now-standard dynamic pressure feedback (DPF) load stabilization mechanism and high-performance multistage servocontrol (Figure 2.2). While the Saturn IB had used electrical position feedback, the mechanical feedback design of the Saturn V actuators was chosen for its superior reliability and environmental robustness.

Based on experience developing TVC for the Jupiter IRBM, MSFC had determined that simple gain stabilization of the load resonance; that is, the pendulum mode of the closed-loop TVC system, was infeasible. Interaction of the engine mode with the autopilot and other proximal structural modes could lead to a risk of coupled instability at the required autopilot performance (e.g., gain) levels. The dynamic pressure feedback valve assembly was a hydromechanical filter network that added lead to the system, introducing a servovalve displacement that was out of phase with the sensed load force and helping to actively damp the load. Significant improvements in TVC performance and robustness were realized as a result of this scheme, and this technology would become the standard for high-performance servoactuators for essentially all subsequent NASA vehicle development programs including the Space Shuttle.

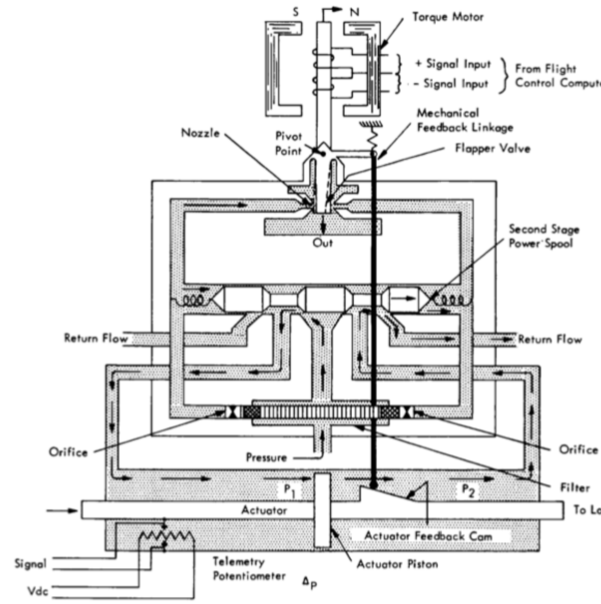

Fig. 2.2: Saturn Servovalve Flow Schematic (*Reproduced from NASA MSFC IV-4-401-1*)

The Saturn IVB third stage auxiliary propulsion system (APS) provided roll control during third stage powered flight, since the two-degree of freedom single engine could only exert pitch and yaw torques for flight control. In addition, the APS was used to effect 3-axis stabilization during orbital coast prior to the translunar injection burn, as well as axial thrust for ullage settling maneuvers. APS thrust control was effected by a quad-redundant series-parallel configuration of on-off oxidizer and fuel poppet valves, arranged such that single-fault electronics and/or valve failures could not affect normal system operation. It is notable that this configuration mitigated the failure modes experienced on Gemini VIII, where an apparent wiring fault caused a thruster to fail to the "on" state, nearly leading to loss of the mission and crew.[8]

2.5 Crew Interface

In general, the level of crew interface capability with the Saturn V launch vehicle far exceeded that which had been provided on the Mercury and Gemini spacecraft for the Mercury-Redstone, Mercury-Atlas, and Titan II GLV. Whereas the Mercury and Gemini spacecraft provided only basic monitoring and abort functionality, the Apollo crew were capable of inhibiting/enabling various modes, sending commands to the LVDC, and facilitating more detailed monitoring of the stage performance, particularly during on-orbit checkout of the S-IVB prior to TLI.

The Saturn V EDS was interfaced with crew displays to provide abort recommendations to the space-

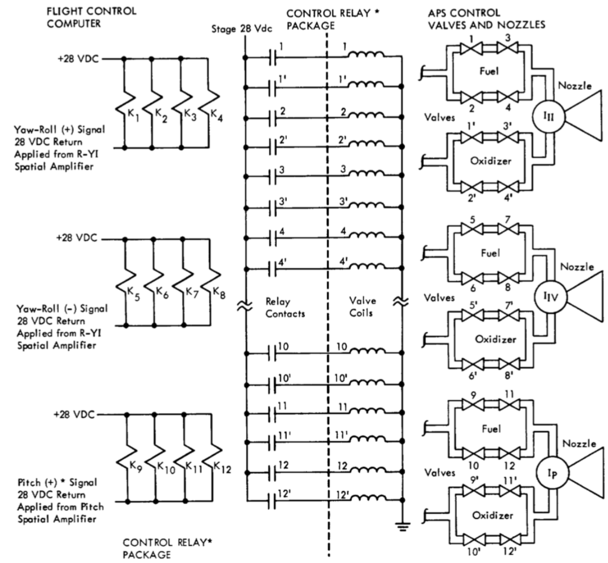

Fig. 2.3: Saturn APS Valve Driver Schematic (Opposing Nozzles Identical) (*Reproduced from NASA MSFC IV-4-401-1*)

craft for other failures, including loss of guidance reference (ST-124 platform failure), engine out (under certain conditions), excess angle of attack, loss of propellant tank ullage pressure, or failure to stage. Inertial platform failure could also be mitigated via a transition to spacecraft manual steering commands during S-II and S-IVB burn, depending on mission rules.[3] In this mode, the crew rotational hand controller (RHC) was used to issue angular increment commands to the LVDC, using the spacecraft IMU as an inertial reference. Flight control loop closure and autopilot functions were still maintained on the Saturn vehicle in this mode using the flight control rate gyros. Manual steering was not available to the crew during S-IC flight; while numerous backup capabilities had been considered, detailed studies had indicated decreased reliability and an unacceptable tendency to exceed bending moments during atmospheric flight if pilot inputs were included in the command path.[9] Similar analyses have influenced the manual commanding rationale for the Space Launch System program.

3. Saturn Flight Dynamics Analysis

The design and flight certification of the Saturn V relied upon first principles methods for the analysis of the vehicle dynamics during ascent, using a hybrid analog/digital simulation scheme and quasi-linear models of the flight dynamics. The formulation used for flight control design and analysis was a planar perturbation method developed with respect to a gravity-turn equilibrium trajectory, as documented in the now well-known paper by Frosch and Vallely.[10] This formulation, and others based on similar principles, were an active area of research at the time in both NASA and the Air Force in the support of multiple ICBM programs, including the Atlas and Titan missile families. Research in this area in the mid- to late 1950s systematized the approach of perturbations with respect to a gravity turn, the use of modal superposition for the assessment of bending stability, and the use of mechanical analogs for propellant sloshing dynamics. While many of these techniques followed directly from rigorous methods already in use for aircraft, the nuances of launch vehicle flight dynamics were not consolidated within the community of practice until the late 1960s, as evidenced by the widespread and simultaneous development of similar approaches in support of various programs.

The equations of motion presented in Frosch and Vallely appear without reference in transfer function form, and are analogous to those presented by Greensite[11] and Lukens *et al.*[12] To the best of the recollection of the original author, the formulation used for Saturn V analysis and presented in Frosch and Vallely was independently derived by Rheinfurth and Hosenthein;[13] these are presented in part in the compilation by Garner.[14]

In what are now referred to in the launch vehicle dynamics community as *standard methods*, the dynamic equations are formulated via superposition using an "integrated body" approach. In this formulation, the orthogonal vibration modes are elicited from a finite element model containing all of the vehicle mass, including the gimbaled engines. After diagonalization, the rigid body degrees of freedom, as well as some of the other dynamic modes, are replaced with a higher-fidelity set of equations that capture effects that cannot be modeled accurately using the finite element method, for example, lateral slosh mode damping that varies as a function of flight condition. In the development of the standard equations, the inclusion of all of the vehicle mass in the finite element model and a choice of coordinate frame origin coincident with the center of mass simplifies the derivation and implementation of the coupled equations of motion.

The fundamental assumptions of this type of perturbation model are as follows:

1. The inertial frame is that of a flat, non-rotating earth, fixed at the launch site at the time of launch.

2. The equations of motion are derived in a rotat-

ing frame, coincident with the rigid body, whose origin is the unperturbed center of mass of the integrated system.

3. The vehicle ascends on a gravity turn trajectory where the angular rate is related to the velocity such that the angle of attack is zero in a quiescent atmosphere. The time history of the angular rates and the associated inertial-to-body kinematic angles are chosen such that the equilibrium body acceleration is collinear with the thrust axis of the vehicle.

4. The equations of motion are integrated in a trajectory frame aligned with the body axes at the linearization equilibrium condition. The kinematic rate of change of this frame is negligible; that is, the angular rate of the trajectory frame with respect to the launch site (the pitch rate along the gravity turn) is small and can be neglected.

5. The vehicle parameters are constant in time.

Such a model yields a relatively compact description of the system equations that can be readily assessed using standard linear system methods in order to elicit the frequency response and thus the stability properties, subject to the foregoing limitations. Since the system is inherently time-varying, the linearized transfer functions are computed at successive time-points along the trajectory and an assumption is made that stability can be assessed by considering points on the trajectory where the parameters are varying "slowly enough" that they may be assumed constant. The approach provides for some quantitative measure of control performance with respect to the evolving trajectory. Although this technique has been the subject of much debate by control theorists in search of Lyapunov functions, the approach has served the aircraft, missile, and launch vehicle community well for over fifty years.

3.1 *Propellant Slosh*

A significant amount of resources were dedicated to the study of the emerging phenomenon of booster propellant slosh, which was just beginning to be well-understood at the onset of the Saturn program in 1961. It was well-known that a mechanical analog could be used to simulate the response of a liquid under moderate to high accelerations, but the detailed analysis and parameterization of such models, particularly with respect to the use of hardware damping mechanisms, was developed in support of the Saturn program. Key contributions by Miles, Bauer, and Dodge, among others, are documented in the NASA compendium SP-106.[15] At the onset of the program, it was assumed that now-unusual techniques for high-g slosh propellant management, such as floating cans, sector compartmentalization, and accordion baffles (as used in Saturn IB) were the most credible solutions to the pressing slosh dynamics problem.[16] As the development of the Saturn V proved, ring baffles were the most simple and analytically tractable choice for slosh suppression, and this approach has been essentially universal for liquid propellant launch vehicle designs ever since.

Fortunately, such arrangements are fairly easy to model and assess in simulations, taking the form of the simple spring-mass-damper for small perturbations of the liquid free surface about its equilibrium position; baffle damping is reasonably approximated using the closed-form Miles equation, although modern simulations rely on computational fluid dynamics (CFD) techniques to overcome limitations in the damping predictions for tank domes and large wave amplitudes. Bauer[17,18] extensively investigated the stability of a rocket-propelled vehicle under closed-loop control with slosh, developing the incredibly useful "danger zone" concept that relates the position of the equivalent slosh mass to the vehicle's instantaneous center of mass and center of percussion. This technique, based on the Routh-Hurwitz criterion for a linearized vehicle, accurately predicts whether a propellant mode will be stable or unstable with feedback control. It is used early in the design process to inform vehicle concepts and set expectations for the allocation of slosh baffle mass.

Similar important contributions in the area of nonlinear and microgravity propellant slosh were realized in the Saturn program, particularly in the area of high-g, nonlinear slosh and low-g propellant management, the latter being crucial to the successful restart of the Saturn IVB to facilitate translunar injection. In fact, nearly an entire test flight (Saturn IB AS-203) was dedicated to assessing on-orbit propellant dynamics, and these data are still used in the validation of CFD codes for the prediction of cryogen behavior in microgravity.

3.2 *NASA FRACTAL and Space Launch System*

It was not until the last two decades that a formal, comprehensive approach to booster flight mechanics modeling came into standard practice in the NASA community, inspired by the disparate approaches to perturbation flight dynamics appearing in the literature. In part, the Frosch and Vallely model, despite its implicit assumptions and limitations, is quite comprehensive and contains most of the terms needed to capture the salient dynamics of a large, ascending booster. The FRACTAL (Frequency Response Analysis and Comparison Tool Assuming Linearity) model was developed at NASA MSFC during the Constellation program using a rigorous, matrix-vector Lagrangian derivation of the equations of motion that reduces to the Saturn V flight dynamics as a special case.[19] This model, now having been extensively verified using both Ares I-X and Space Shuttle models and flight data, is a Space Launch System program critical math model (CMM), integrated with numerous numerical and post-processing tools to provide a comprehensive capability for large booster flight control system design optimization.

FRACTAL approaches the assertion that an accelerating, trajectory-relative frame is approximately inertial using a method based upon the Boltzmann-Hamel equations.[20] Here, the *nonholonomic* generalized velocities are body-referenced velocity $\mathbf{v}$ and the body angular rates ω, and the linearized equations describe perturbations along a particular solution of the boundary value problem arising from the Lagrangian; *viz.*, the motion equations. The ultimate goal is a set of linear equations describing the perturbation dynamics with respect to a rigid-body trajectory $\mathbf{v}_0(t)$, $\omega_0(t)$, not the trajectory itself. If the operating point for the dynamic analysis is taken to be about a trivial solution, or constant generalized velocity, this distinction is irrelevant, but in the case of a launch vehicle dynamic analysis, linearization is with respect to a *solution* of the nonlinear motion equations.

A key distinction is as follows. In the dynamic analysis, it is common to encounter the skew-symmetric product of velocities in the form $\omega^\times \mathbf{v} \in \mathbb{R}^3$. Considering perturbations about a trajectory,

$$\begin{aligned}\omega^\times \mathbf{v} &= (\omega_0 + \delta\omega)^\times (\mathbf{v}_0 + \delta\mathbf{v}) \\ &= \omega_0^\times \mathbf{v}_0 - \mathbf{v}_0^\times \delta\omega + \omega_0^\times \delta\mathbf{v} + \delta\omega^\times \delta\mathbf{v}.\end{aligned}$$

This expression contains one zero-order term, two important terms of order one, and one term of order two. The equilibrium angular rate is usually small and can be assumed zero; this considerably simplifies the development. However, the first-order term containing $\mathbf{v}_0$ can be significant; for a launch vehicle or missile, both the velocity and its time derivative can be large. From this time derivative arise important effects such as sloshing propellant and engine offset moments that, in the past, were added *ad hoc.* More importantly, the proper transformation of the aerodynamic partial derivatives to trajectory-relative coordinates on a gravity turn trajectory can only be recovered through perturbation expansions. Through these more rigorous procedures, the complete linear perturbation equations can be recovered with fewer assumptions and limitations than the earlier formulations.

The FRACTAL model also extends the Saturn-era approach with a particular focus on engine dynamics and servoelastic effects, an area to which the Saturn V stages were not particularly sensitive but has been shown to be of more concern for configurations such as Space Launch System. The presence of a servoactuator position control loop substantially changes the character of the engine dynamic (pendulum) modes, and this effect can strongly couple with the global vehicle bending. It is advantageous to replace the engine dynamics with a model that accurately represents the response of the coupled engine-servo system not only to position commands but also to external load torques that result from coupling with the vehicle; so-called tail-wag-dog (TWD) and dog-wag-tail (DWT). The traditional integrated body approach places special requirements on the finite element model so as to eliminate degrees of freedom that will later be replaced by higher-fidelity models, that is, the residual engine pendulum modes. Compared with Saturn-era models, modern finite element models contain many millions of degrees of freedom; they trade fidelity for an unfortunate and inevitable (although cost-saving) reduction in test-based validation. Since these models cannot be arbitrarily and ideally constrained, it is often impossible to generate an appropriate set of modes without a sacrifice in fidelity elsewhere in the model.

FRACTAL instead implements a fully-coupled explicit formulation of the *reduced-body* approach, where a truncated set of orthogonal modes of a finite element model is coupled in such a way that the compliance of the engine-actuator backup structure can be accurately captured. This allows the direct and simultaneous solution of the equations representing dynamic coupling of the engine and global bending structure, but the local engine and backup structure compliance remains within the servoactuator model. Thus, the local thrust structure dynamics can be partitioned from the global vehicle bending modes and represented with fidelity appropriate to that subsystem.

4. Saturn Flight Control Design

The Saturn V flight control system relied on a minimum complexity approach using proportional-derivative feedback and low-order, linear analog bending filters. As is typical in the development of new vehicles, several advanced concepts including adaptive control and nonlinear filter techniques were explored during the course of the vehicle development, but ultimately the architecture flown was that having the minimum complexity that was able to satisfy the flight control requirements. Considering that the design was implemented in analog hardware using relays, passive filter networks, and servomechanical gain changers (in the case of Saturn IB), the minimum complexity design also offered the lowest cost and most reliable solution.

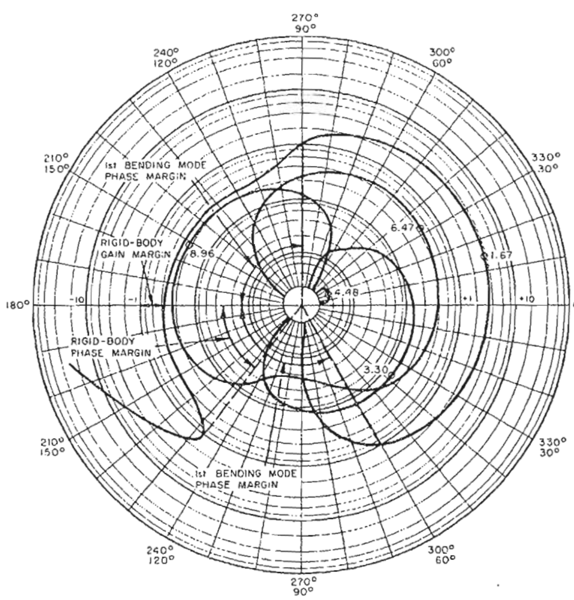

Fig. 4.1: Saturn S-II Open-Loop Frequency-Domain Analysis (*Reproduced from Ref. 21*)

The Saturn program standardized guidelines for the development of large booster flight control systems. Whereas prior vehicle development programs had relied more heavily on root locus techniques and the assessment of absolute linear stability, emerging computer capability for the computation of frequency response allowed more focus on the Nyquist theorem and the use of linear stability margins to predict the performance of the closed-loop system with sloshing and bending modes included. The use of worst-on-worst tolerance analysis in linear control system assessment was combined with analog time-domain simulations to estimate performance statistics, particularly with respect to wind loads.[21] For the first time, it became practical to simultaneously assess the frequency response of multiple sets of dispersed vehicle parameters so as to compute the worst-case stability margins.[‡]

The stability margin guidelines used in the Saturn program were an extension of the typical ± 6 dB gain margin and 30 degrees phase margin that follow from basic servomechanism control theory, with additional conservatism allocated to the phase-stabilized first bending mode. Typical tolerances on key parameters included a 10-foot variation in the center of pressure location, a 10% variation in the fundamental lateral bending mode frequencies, a 3% variation in thrust, and a 10% variation in the effective control gains, owing to analog component tolerance effects.[6,10]

The low bending frequencies of the Saturn configurations, and the limited filter order of the analog hardware implementation, necessitated the use of active (phase) stabilization to mitigate the risk of control-structure interaction. In a counterpoint to the challenge of control-structure interaction, the vehicle was aerodynamically unstable for most of the flight, requiring active attitude error feedback for stabilization. The first bending mode occurred close to 1 Hz, forcing the difficult trade between autopilot bandwidth required for rigid-body stability and the margins required for robust decoupling of the vehicle dynamics and the flight control loop. Gain scheduling in the Saturn V S-IC did not rely on any external sensing mechanisms but rather a switch selector command driven by the time-based sequencing logic.[22] In the final design, a single switchpoint occurred at 100 seconds after liftoff, which ensured adequate margins throughout flight. APS control for S-IVB roll and 3-axis on-orbit stabilization was performed using an attitude-attitude rate phase plane technique (Figure 4.2). While not as fuel optimal as the disturbance observer approach employed on the Apollo LM,[23] it was able to meet flight control requirements with minimum complexity. This type of linear switch curve became standard practice in the 1960's and is still used for most boost vehicle RCS designs.[24]

‡In a 2009 interview, responding to the author's claims of novelty in using MATLAB to automatically present multiple Nichols charts on the same axes, Mr. Vallely[10] noted that Saturn flight control engineers had simply printed the results on transparencies and stacked them together.

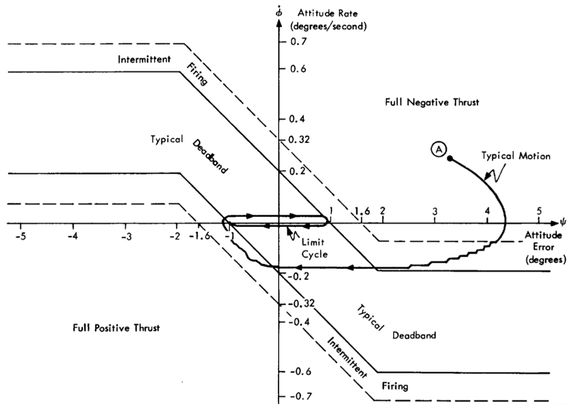

Fig. 4.2: Saturn APS Phase Plane Design (*Reproduced from NASA MSFC IV-4-401-1*)

The Saturn V, with its multiple propellant tanks and densely spaced sloshing modes, demonstrated that a robust and high-performance autopilot could be implemented for a massive vehicle with minimum complexity, i.e., proportional-derivative control and a fifth-order passive analog filter network. Due in part to the exceptional overall system balancing and uncertainty control, particularly in the TVC actuators, such a design was readily achievable with the applied efforts of experienced MSFC flight control engineers. For better or worse, this success seems to have limited system engineers' enthusiasm for deploying advanced control systems on large rockets in the decades that followed.

4.1 Load Relief

A significant development of the Saturn vehicles was the emergence of a design process for launch vehicle in-flight load relief algorithms. Employing concepts previously explored for the control of aircraft longitudinal maneuvers using normal acceleration feedback, the load relief algorithm was an attempt to reduce bending loads - and therefore required structural mass - by allowing the vehicle to sense and adjust to changes in wind velocity along the trajectory. Hoelker[25] provided a treatment a generic load-relief equipped attitude control system by augmenting the well-known PD control system with body-mounted accelerometer feedback or angle of attack feedback. In addition to illustrating the equivalence of an autopilot realization that uses the ideal angle-of-attack feedback to that achieved via a body-mounted accelerometer, Hoelker introduced four canonical forms of load relief corresponding to specific control objectives and developed the specific gain relationships for each. This rigid body elucidation of the accelerometer-based load relief has provided the basis for the framework and parameter selection of the basic load relief control law utilized on Saturn, Shuttle,[26,27] Ares I-X, Ares I,[28] and now SLS.[29]

While ultimately not employed on the Saturn V, the accelerometer-based load relief algorithm was extensively flown on the Saturn IB, where it was demonstrated to provide a significant advantage in the reduction of trajectory-relative error and structural loading due to gusts and wind variability. The Saturn V vehicle was shown, conversely, to realize fewer benefits of the load relief algorithms, in part due to a lack of correlation between the quasi-steady load metrics and the actual transient bending moments. In addition, the Saturn V exhibited lower frequency bending modes that nearly overlapped the control system bandwidth and thus required significant attenuation in the extreme forward mounted accelerometer path. The necessary accelerometer filtering for the Saturn V configuration was difficult to achieve, and a contributing factor was difficulty in fabricating an accelerometer filter with the appropriate low-frequency characteristics using analog components that met the packaging, tolerance, and stability requirements of the Saturn FCC. Furthermore, the deletion of load relief eliminated the use of the cam-driven gain scheduler mechanism as used in the Saturn IB FCC, increasing reliability of the analog flight control system.

4.2 Space Launch System Flight Control

The Space Launch System (SLS) is NASA's next-generation exploration-class launch vehicle for large-scale crewed and uncrewed space access, including such objectives as human transit to Mars, rendezvous with near-earth asteroids, and the launch of unmanned probes to distant solar system targets such as Europa. Its design provides for a level of performance and reliability that is unmatched in any existing or planned launch system, including an ability to loft approximately 57,000 lbm to trans-lunar injection (TLI) in its initial Block 1 configuration (Figure 4.3). Its evolved configurations, Block 1B and Block 2, utilize the Exploration Upper Stage (EUS) to substantially increase performance. The Block 1B with EUS has a cargo payload performance capability of approximately 88,000 lbm to TLI. The Block 2, more than 375 feet long and using upgraded solid rocket motors (SRMs), is able to loft 290,000 lbm to low Earth orbit (LEO) or 99,000 lbm to a heliocentric orbit. These capabilities place the SLS in a category of performance commensurate with that of the Saturn V.

The SLS leverages hardware, processes, and design concepts derived from the Saturn and Space Shuttle programs, including an 27.5 ft diameter core stage

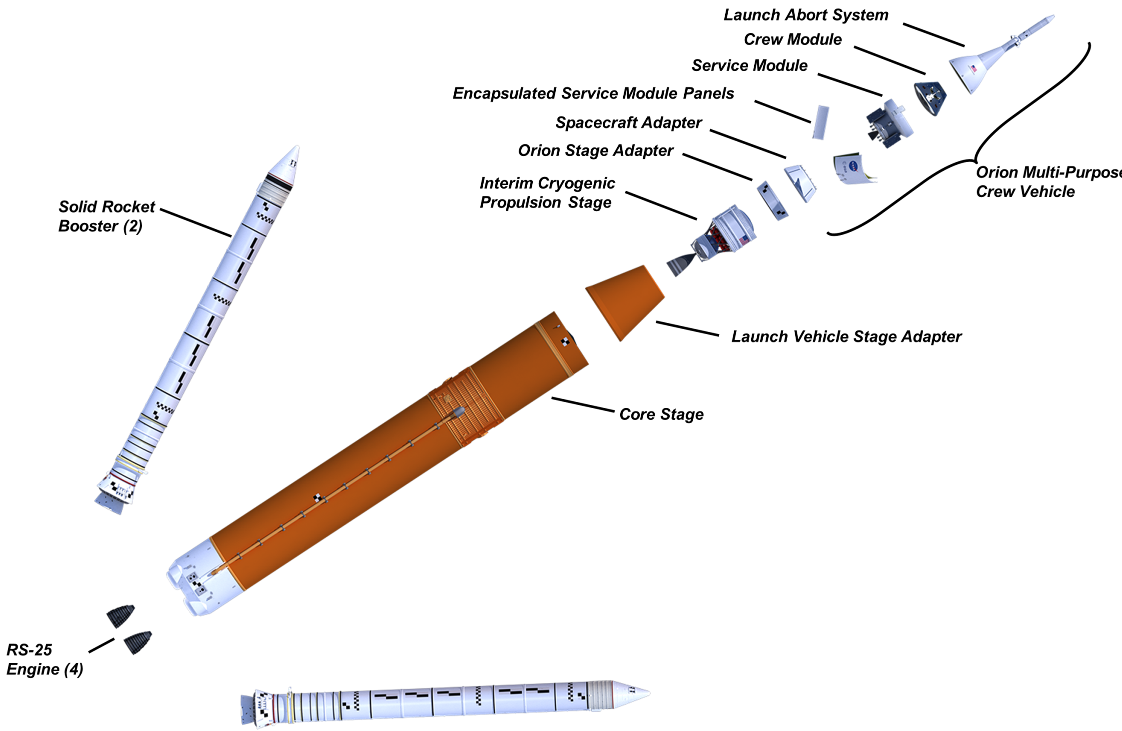

Fig. 4.3: Space Launch System Block 1 Configuration (NASA)

containing more than 700,000 gallons of cryogenic propellants.[30] The core stage is powered by four RS-25E liquid engines derived from the highly successful Space Shuttle Main Engine (SSME), each producing about 475,000 lbf of thrust.[31] Additional thrust is provided by two 5-segment Reusable Solid Rocket Motor-V boosters (RSRMVs). Each RSRMV provides a peak sea level thrust of about 3.3 million lbf and provides primary ascent propulsion during the 126-second boost phase. Three-axis control and stabilization during powered flight is provided by coordinated thrust vectoring of the solid rocket nozzles as well as all four RS-25E core stage engines, using 12 pressure feedback stabilized, quad-redundant precision hydraulic actuators. These actuators, initially developed for the Space Shuttle program, are a direct evolution of the actuator technology discussed in Section 2.4.

An overview of the SLS GN&C architecture is shown in Figure 4.4. The core flight control algorithms consist of (1) a gyro blender that optimally weights rate measurements from multiple rate gyro stations, (2) an array of linear bending filters that provide frequency-domain shaping to provide active or passive stabilization of vehicle bending and sloshing dynamics, (3) a proportional-integral-derivative control law, (4) angular disturbance compensator and in-flight load relief algorithms, (5) an on-line gain adaptation algorithm, and (6) a real-time multi-effector control allocation law.

The present architecture is a direct evolution of that used on the Saturn V, relying on the basic proportional-derivative control with an additional integral function, which produces bias compensation signals to mitigate effects such as thrust vector misalignment. The use of rate gyro blending was found to be unnecessary in the Saturn V configuration, whereas the Space Launch System employs a set of three redundant Rate Gyro Assemblies (RGAs) located in the forward skirt, intertank region, and aft skirt. Pitch and yaw body rate measurements from these sensors are optimally combined using a robust set of blending gains to maximize the rejection of sensed bending dynamics. In the present application, the various configurations admit either active (phase) or passive (gain) stabilization, using the same techniques as originally demonstrated on the Saturn V. A numerical optimization technique is utilized to design structural filters that provide maximum robustness to structural mode uncertainty while minimizing phase lag at critical control system and sloshing mode frequencies. In contrast to the passive filter networks of the Saturn FCC, the SLS bending filters are implemented in software as digital, 8^{th}-order filter

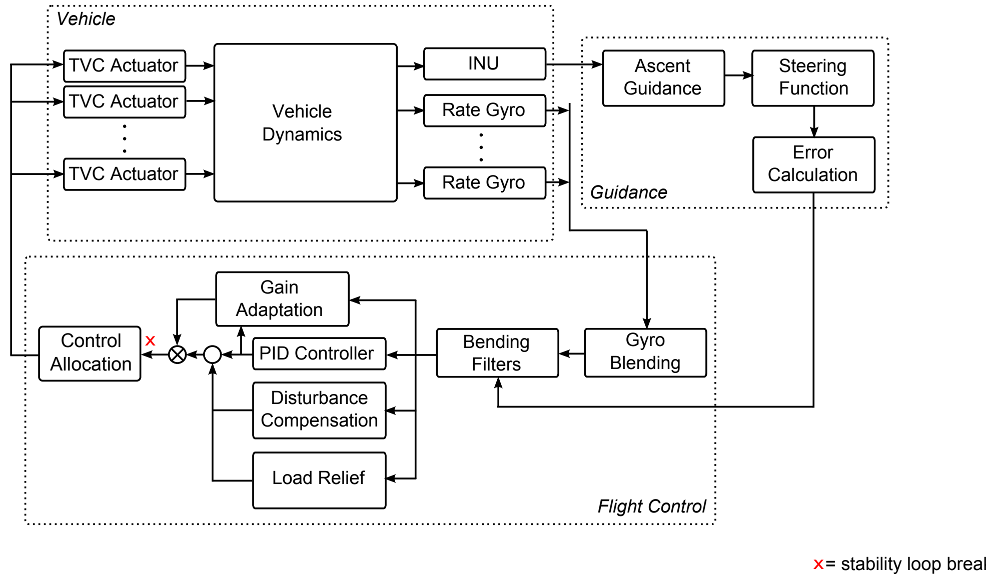

Fig. 4.4: SLS GN&C Top-Level Architecture

banks executing at an update rate of 50 Hz. However, the target design guidelines (e.g., stability margins), parameter uncertainty values, and methodology used for the SLS design - particularly with respect to active stabilization of bending - are derived from Saturn V flight control experience.

During the development of the flight control designs for both the Constellation and SLS programs, the Saturn load relief architectures provided a guide towards achieving an optimal balance of load reduction, attitude control, and trajectory drift objectives. SLS employs a generic form of the load relief algorithm, carrying its nearest roots in the Ares IX and Ares I autopilots. Its formulation extends its applicability to basic disturbance rejection throughout the ascent flight regime. Through the now well-established means of digital flight control and the ability to rapidly optimize large multivariable systems, achievement of the necessary high performance attenuation filters for the load relief function carries little of the Saturn-era implementation barriers. However, due to the similarity of the SLS vehicle configuration to the Saturn V, the achievable bandwidth of load relief is ultimately also limited by the stability considerations treated so thoroughly in the Saturn era of development.

Two notable improvements in the SLS architecture are the use of an advanced control allocation scheme, as well as the inclusion of an adaptive element. The former is used to optimally effect moments about the vehicle center of mass, considering the differences in geometry, thrust, and control capability of the solid rocket boosters and core stage engines. This algorithm also maintains control authority in the event of a loss of engine thrust, improving margins and maintaining performance.

The adaptive element is a simple adaptive gain law that acts as a supplemental mechanism to improve robustness to uncertainty in the vehicle dynamics. In order to fully realize the benefits of an adaptive element, the adaptive law has been carefully refined to specifically address the failure modes and uncertainties associated with launch vehicles. Its design and analysis is treated extensively elsewhere.[32,33]

Typical stability margin criteria used during the design process are consistent with those used for the Saturn V and the Space Shuttle. Stability criteria are evaluated both for the nominal parameter set (as design goals) and via uncertainty models using Monte Carlo methods. Stability criteria associated with dispersed (uncertain) models are lower than those associated with the nominal system, but are nonzero so as to ensure a level of residual conservatism even after all uncertainties are applied. An elliptical closest approach (disc margin) criteria, derived from the classical stability margin criteria, is applied to maximize robustness to simultaneous perturbations in gain and phase uncertainty.

The design criteria applied to the SLS vehicle flight control design are summarized in Table 4.1. A wide variety of flight control analyses depend on the high-fidelity FRACTAL software capability discussed in Section 3.2.

Vehicle Type	Response Type	Rigid Body	Slosh (Phase Stabilized)	Slosh (Gain Stabilized)	Bending (Gain Stabilized)
Nominal	Nichols Disc Margin	Ellipse with axes ±30 deg and ±6 dB			
	Peak Amplitude	N/A	< +10 dB	N/A	< -10 dB
Dispersed	Nichols Disc Margin	Ellipse with axes ±20 deg and ±3 dB			
	Peak Amplitude	N/A	N/A	N/A	< -6 dB

Table 4.1: SLS Stability Margin Criteria

5. Conclusions

The Saturn V GN&C analysis processes, subsystem architecture, and design approach have had a lasting impact on the development of flight dynamics and control technology within the NASA launch vehicle community. Fundamentals of basic autopilot architecture and design guidelines were brought forward into the current community of practice, where their successes, failures, advantages, and limitations were leveraged to minimize costs and accelerate development of the Space Shuttle, the Ares family, and now Space Launch System. Advanced techniques and the incredible breadth of subsystem test experience, continue to be of paramount importance in building confidence in a much different, cost-constrained development environment.

The authors have been privileged to have had as mentors during the Constellation program many of the key contributors to the development of the Saturn vehicles' GN&C technology as they approached the end of their careers at NASA Marshall Space Flight Center. The magnitude of their accomplishments during the Saturn program in the course of less than a decade cannot be overstated. The Space Launch System flight controls discipline has built upon this deep legacy of NASA experience to develop a set of tools, algorithms, and processes that will support the SLS program, as well as future launch and space transportation vehicle concepts, throughout the next generation of human spaceflight operations.

Acknowledgements

The authors would like to thank Mr. F. Brooks Moore, Mr. Pat Vallely, Mr. Charles Cornelius, and Dr. Robert Ryan for their technical contributions, systems insight, and mentorship in the years leading up to the development of Space Launch System.

References

[1] Bilstein, R., Stages to Saturn: A Technological History of the Apollo/Saturn Launch Vehicles, NASA SP-4206, 1980.

[2] NASA TM X-881, "Apollo Systems Descriptions, Vol. II," NASA Marshall Space Flight Center, February 1964.

[3] NASA MSFC-MAN-507, "Saturn V Flight Manual, SA-507," NASA Marshall Space Flight Center, August 1969.

[4] NASA MPR-SAT-FE-69-9, "Saturn V Launch Vehicle Flight Evaluation Report AS-506, Apollo 11 Mission," September 1969.

[5] NASA MSFC-IV-4-401-1, "Astrionics System Handbook, Saturn Launch Vehicles," NASA Marshall Space Flight Center, November 1968.

[6] Haeussermann, W., "Description and Performance of The Saturn Launch Vehicle's Navigation, Guidance, and Control System," NASA TN D-5869, NASA Marshall Space Flight Center, July 1970.

[7] Von Der Porten, P., and Ahmad, N., "PEG Enhancement for EM1 and EM2+ Missions," American Astronautical Society Guidance, Navigation, and Control Conference, Breckenridge, CO, February 2018, AAS 18-136.

[8] NASA MSC-G-R-66-4, "Gemini Program Mission Report (Gemini VIII)," NASA Manned Spacecraft Center, April 1966.

[9] Hardy, G., "Man's Role in Launch Vehicle Guidance and Control," AIAA Guidance, Control, and Flight Mechanics Conference, Princeton, NJ, AIAA 69-876, August 1969.

[10] Frosch, J. and Vallely, D., "Saturn AS-501/S-IC Flight Control System Design," J. Spacecraft, Vol. 4, No. 8, 1967, p. 1003-1009.

[11] Greensite, A., "Analysis and Design of Space Vehicle Flight Control Systems, Volume I – Short Period Dynamics," NASA CR-820, 1967.

[12] Lukens, D., Schmitt, A., and Broucek, G., "Approximate Transfer Functions for Flexible-Booster-and-Autopilot Analysis," USAF WADD-TR-61-93, 1961.

[13] Rheinfurth, M., "Control-Feedback Stability Analysis," Army Ballistic Missile Agency, DA-TR-2-60, 1960.

[14] Garner, D., "Control Theory Handbook," NASA TM-X-53036, 1964.

[15] Abramson, H., "The Dynamic Behavior of Liquids in Moving Containers," NASA SP-106, 1966.

[16] Bauer, H., "Propellant Sloshing Problems of Saturn Test Flight SA-1," NASA MTP-AERO-62-29, NASA Marshall Space Flight Center, March 1962.

[17] Bauer, H., "Fluid Oscillations in the Containers of a Space Vehicle and Their Influence Upon Stability," NASA TR R-187, NASA Marshall Space Flight Center, February 1964.

[18] Bauer, H., "Stability Boundaries of Liquid-Propelled Elastic Space Vehicles with Sloshing," J. Spacecraft, Vol. 3., No. 2, February 1966, p. 240-246.

[19] Orr, J., "A Flight Dynamics Model for a Multi-Actuated Flexible Rocket Vehicle," AIAA Atmospheric Flight Mechanics Conference, Portland, OR, AIAA-2011-6563, August 2011.

[20] Hughes, P., Spacecraft Attitude Dynamics, Dover, 2004.

[21] Ryan, R. and King, A., "The Influential Aspects of Atmospheric Disturbances on Space Vehicle Design Using Statistical Approaches for Analysis," NASA TN D-4963, NASA Marshall Space Flight Center, January 1969.

[22] Haeussermann, W. and Duncan, R., "Status of Guidance and Control Methods, Instrumentation, and Techniques as Applied in the Apollo Project," Advisory Group for Aeronautical Research and Development, North Atlantic Treaty Organization (NATO), Duesseldorf, Germany, October 1964.

[23] Widnall, W.S., "Lunar Module Digital Autopilot," J. Spacecraft, Vol. 8, No. 1, January 1971, p. 56-62.

[24] Hall, R., *et al.*, "Design and Stability of an On-Orbit Attitude Control System Using Reaction Control Thrusters", AIAA Guidance, Navigation, and Control Conference, AIAA SciTech Forum, AIAA 2016-0087

[25] Hoelker, R.F., "Theory of Artificial Stabilization of Misses and Space Vehicles with Exposition of Four Control Principles," NASA TN D-555, NASA Marshall Space Flight Center, June 1961.

[26] Ryan, R., "Fundamental Concepts of Structural Loading and Load Relief Techniques for the Space Shuttle," NASA TM X-64684, NASA Marshall Space Flight Center, August 1972.

[27] Schleich, W., "The Space Shuttle Ascent Guidance and Control," AIAA Guidance and Control Conference, San Diego, CA, August 1982, AIAA 82-1497.

[28] Jang, J., *et al.*, "Ares I Flight Control Design," AIAA Guidance, Navigation, and Control Conference, Toronto, Ontario, Canada, August 2010, AIAA 2010-8442.

[29] Orr, J., Wall, J., VanZwieten, T., and Hall, C., "Space Launch System Ascent Flight Control Design," American Astronautical Society Guidance, Navigation, and Control Conference, Breckenridge, CO, February 2014, AAS 14-038.

[30] Donahue, B., "The Space Launch System: Development Progress," AIAA SPACE 2016, AIAA SPACE Forum, Long Beach, CA, September 2016, AIAA 2016-5415.

[31] Ballard, R., "SSME to RS-25: Challenges of Adapting a Heritage Engine to a New Vehicle Architecture," Proc. Sixth European Conference for Aeronautics and Space Sciences (EUCASS), Krakow, Poland, June 2015.

[32] Wall, J., Orr, J., and VanZwieten, T., "Space Launch System Implementation of Adaptive Augmenting Control," American Astronautical Society Guidance, Navigation, and Control Conference, Breckenridge, CO, February 2014, AAS 14-051.

[33] NESC-RP-14-00964, "Stability of the Space Launch System (SLS) Flight Control System (FCS) with Adaptive Augmentation," NASA Engineering and Safety Center, July 2016.